Research Journal of Chemical Sciences ISSN 2231-606X
Vol. **14(2),** 25-31, June **(2024)** *Res. J. Chem. Sci.*

Heterogeneous Fenton processes for the degradation of methylene blue in aqueous solution: Application of composite biochar doped with magnetite

Abdoul Ntieche Rahman[1*], Gervais Ndongo Kounou[2], Sakué Ngankam Eric[1], Kouotou Daouda[2], Tamafo Fouegue Aymard Didier[1] and Abdelaziz Baçaoui[3]

[1]Department of Chemistry, Higher Teacher Training College Bertoua, The University of Bertoua, PO Box 652, Bertoua, Cameroon
[2]Physical and Theoretical Chemistry Laboratory, Department of Inorganic Chemistry, Faculty of Science, University of Yaoundé I, Yaoundé, Cameroon
[3]Department of Chemistry, Faculty of Science Semlalia, University of Cady Ayyad, Marrakech, Morocco
rahmino@gmail.com

Available online at: www.isca.in, www.isca.me
Received 18th February 2024, revised 1st March 2024, accepted 2nd May 2024

Abstract

The degradation of methylene blue (MB) in aqueous solution by heterogeneous Fenton process using two synthetized materials was investigated. One is a biochar material namely PB_1P_15 derived from banana peels-plastic bottles composite and another is a magnetized biochar material namely PB_1P_15M synthetized by co-precipitation of iron III chloride hexahydrate ($FeCl_3.6H_2O$) and iron II chloride tetrahydrate ($FeCl_2.4H_2O$) of the aforementioned biochar. The two synthetized materials were characterized by X-ray diffraction (XRD), scanning electron microscopy (SEM-EDX), Fourier transformed infrared (FTIR) and Brunauer-Emmett-Teller / Barret-Joyner-Halenda (BET/BJH) techniques. The characterization analyses revealed successively, the appearance of reverse spinel groups of magnetite, elongation vibration of Fe-O bonds and specific surfaces areas of 83.03m^2/g to 163.9m^2/g for biochar (PB_1P_15) and diochar/Fe_3O_4 (PB_1P_15M) respectively. This prominence presence of iron oxides in the magnetite forms (Fe_3O_4) mainly on PB1P15M surface was used as catalyst for heterogeneous Fenton process for MB degradation. The photo-Fenton analyses tests indicated a strong degradation of MB of 69.7% in dark condition and up to 98.4% in the presence of UV light. These results were obtained under optimum conditions of 80mg/L and pH equals to 2 of MB solution, 0.2mg/L of H_2O_2 solution with 15mg of PB_1P_15M in one hour of contact time. Finally, the catalysts performances were tested by its recovery in MB solution through magnetic separation and reused three times without any loss of activated denoted.

Keywords: Biochar, co-precipitation, degradation, magnetic separation, methylene blue, heterogeneous catalysis.

Introduction

The discharge of dyes from industrial wastewaters in the environment can cause several problems to human beings and living organisms, due to their toxic, mutagenic and carcinogenic characters. Some of these dyes even at very low concentrations are visible and can color a large quantity of water. Thus, the removal of dyes from industrial wastewaters before its discharge into the environment is a real environmental challenge. For this purpose, several methods including, coagulation/flocculation[1], reverse osmosis[2], photochemical degradation[3], membrane filtration[4] adsorption[5], just to name the few have been developed to remove them. However, these aforementioned methods are limited because it only allows the transfer of the dyes from liquid to solid phases, during the process they generated some by-products and; require additional treatment and consequently increase the process cost[6]. Recently, Advanced Oxidation Processes (AOPs), namely heterogeneous photocatalysis, photolysis of peroxide or ozone (H_2O_2/UV, O_3/UV), Fenton or photo-Fenton processes, radio or sonolysis of water, peroxonation and photo-peroxonation (O_3 / H_2O_2 / UV), sonication oxidation process, have been used as emerging destructive methods with complete mineralization of pollutants[7]. AOPs produce enough hydroxide radicals ($HO^\bullet$) to degrade complex and recalcitrant organic pollutants prior to their mineralization.

Many authors have focused their attention on titanium dioxide (TiO_2), as a typical photo-catalyst semiconductor, owing to its excellent features such as strong oxidizing power, higher chemical and thermal stability, less poisoning tendency, cheap and available[8]. However, the problem of separation from the liquid phase and its reuse still remain and limit its application. To overcome these problems, the use of magnetic semi-conductors as catalysts, like magnetite (Fe_3O_4), is in progressively adopted[9]. During the oxidation process using Fe_3O_4 as catalyst, ferric ions (Fe^{3+}) and ferrous ions (Fe^{2+}) ions are involved in the catalytic oxidation cycles through interaction with the oxidant and it exhibited an efficient catalytic activity[10]. Hydrogen peroxide (H_2O_2) easily generates hydroxide radicals ($HO^\bullet$) via the oxidation of Fe^{2+} to Fe^{3+} ions (Equation-1). Subsequently, the reduction of Fe^{3+} ions are done in the presence of water molecules and UV- light, by generating other $HO^\bullet$ radicals (Equation-2)[10]. The $HO^\bullet$ radicals are also

produced from the homolytic breakage of the O-O bonds of H_2O_2 molecules, catalyzed by UV- light (Equation-3).

$$Fe^{2+} + H_2O_2 \longrightarrow Fe^{3+} + HO^{\bullet} + HO^{-} \quad (1)$$
$$H_2O_2 + UV \longrightarrow 2\,HO^{\bullet} \quad (2)$$
$$Fe^{3+} + UV + H_2O \longrightarrow HO^{\bullet} + Fe^{2+} + H^{+} \quad (3)$$

To allow and facilitate electronic transfer, adsorption and reduction of the energy gap of magnetite in order to prevent the recombination of electron holes during photocatalysis; magnetite are impregnated on different supports such as activated carbons[11], carbon nanotubes, clays, biochar[12], microsphere carbons, multi-walled carbon nanotube, graphene and graphene oxides. The conductive nature of biochar electrons can reduce the rapid recombination of the electron pair hole/h+ during the photocatalysis process[13]. The functional groups such as alcohols, acids, ketones, amines, quinones on their surfaces can undergo reversible redox reactions. Co-precipitation method is mostly used for the synthesis of nanoparticle materials of controlled sizes and with magnetic properties. This method favorites production of fine and stoichiometry particles of single and multi-component metal oxides[14].

In the present work, plastic bottles wastes based polyethelene terephthalate (PET) and banana peels (musa) have been used for the preparation of the composite biochar. The idea of using banana peels combined with PET is due to the low yield of the coal based on PET alone. In addition, plastic bottles (PET) are recognized among the most abundant and polluting plastic wastes owing to their low bio and photodegradation. The banana processing industries produce around 40% of waste commonly known as "banana peels". These banana peels are not used and are mostly discharged in large quantities as solid waste[15]. Thus, the mixture of banana peels and plastics bottles to produce a composite biochar seems to be an alternative route to fight against environmental pollution. The composite biochar was impregnated by co-precipitation technique in order to degrade methylene blue via Fenton and photo-Fenton. For this purpose, the effects of contact time, solution pH, initial concentration of MB, catalyst mass and H_2O_2 concentration were thoroughly studied. The reusability and efficiency performances of exhausted catalysts were also assessed.

Materials and Methods

Chemicals used: Iron (III) chloride hexahydrate ($FeCl_3.6H_2O$, 99%) and iron (II) chloride tetrahydrate ($FeCl_2.4H_2O$, 99%) were provided by LaboChemie. Sodium hydroxide (NaOH, ≥ 99%) and ethanol (CH_3CH_2OH, ≥ 99%) were purchased from Sigma Aldrich. Hydrochloric acid (HCl, 37%) came from CarloERBA. Hydrogen peroxide (H_2O_2, 30.1%) came from PROLABO. Methylene blue ($C_{16}H_{18}ClN_3S$, 98%) provided by Reactive RAL. All the above chemicals were of analytical grade and used without further purification.

Preparation of Biochar/Fe_3O_4 composite: The "musa" banana peels and plastic bottles used as precursors were respectively collected in local markets and waterlogged channels of Yaounde city (Cameroon). These precursors were washed several times with tap water to remove all the impurities, then sun dried and followed by washing with distilled water and finally oven dried for 24 hours at 80^0C. Both the two materials were cut into small particles and mixed into a mass ratio of 1:1. The mixture was loaded into the reactor of Carboliteturbular furnace, at 10^0C/ min of heating rate, for a final temperature of 500^0C, then maintained for 120 min residence time, under nitrogen flow rate of 0.15mL/min until the complete cooling of furnace. When the carbonization was achieved, the biochar was collected and stored in the desiccator.

The biochar/Fe_3O_4 composite was prepared by co-precipitation method as described by Monika et al.[16]. Briefly, it consists of introducing 2.0g of the previously prepared biochar in 200mL of an aqueous solution containing 7.32g of $FeCl_3.6H_2O$ (27mM) and 2.67g of $FeCl_2.4H_2O$ (13.5mM) in the ratio of 2/1 (Fe^{3+}/Fe^{2+}). The mixture was then stirred magnetically at 80^0C. 50mL of NaOH solution (5M) was added drop wise while maintaining the temperature at 80^0C and the pH value within the range 6. The obtained suspension was stirred for about 60min until a color change from brown to black. The mixture was allowed to cooling at room temperature, filtered and the precipitate was washed several times with distilled water. The biochar/Fe_3O_4 composite obtained was dried at 80^0C and stored for further analysis. Pure magnetite was prepared by the same procedure in the absence of biochar.

Characterization techniques: Fourier transform infrared (FTIR) spectra were recorded by KBr pellets disc technique (0.09 g of KBr and 0.01 g of adsorbent) with a resolution of $4cm^{-1}$ in the range 4000-400cm^{-1} using Vertex 70 DTGS device. Scanning electron microscopy (SEM) analysis was used to observe the morphology and the local surface composition of adsorbents. The device used was VEGA3 TESCAN coupled with an Energy Disperse X-rays spectroscopy (EDAX TEAM with 125.9eV of resolution) to allow the local elemental composition in different zones of the adsorbents. The analysis of specific surface areas, pore volume as well as particle size distribution was calculated using the Brunauer-Emmett-Teller) BET method by N_2 adsorption/desorption at 77.13K in the micrometric sorptometer model device (Thermo Electron Corporation, Sorptomatic Advanced Data Processing). After N_2 adsorption, the sample is evacuated at 307.13 K. The cumulative volume and surface areas are calculated using Brunauer-Emmett-Teller / Barret-Barret-Joyner-Halenda (BET/BJH) at relative pressures $0{,}05 \leq P/P° \leq 0{,}33$ for adsorption and P/P° = 0.9 for desorption.

Catalysis and Photocatalysis Procedures: The photocatalytic activity of biochar/Fe_3O_4 composite was evaluated on the BM degradation in aqueous solution. For the Fenton process, 50mL of MB solution of 80mg/L was introduced into 200mL conical

flask, then an exact amount of biochar/Fe_3O_4 composite was added followed by a subsequent volume of H_2O_2. The mixture obtained was stirred in dark condition for a few times. For the photo-Fenton process, an exact mass of the photocatalyst was introduced into a 200mL conical flask containing 50mL of MB solution of 80mg/L. The mixture obtained was stirred for 30 min in the dark condition to ensure the adsorption-desorption equilibrium between the photocatalyst and MB solution. After stirring, a certain volume of H_2O_2 was added to the mixture of solution. The conical flask was surrounded by 3 UVA lamps of 15W power, at a wavelength ranging between 345-400nm. After stirring the suspension in a dark condition (Fenton) or under UV-irradiation (photo-Fenton) for several times, 3.0 and 4.0mL suspension were taken out and filtered using a 0.45µm filter or magnetic separation. The MB concentration of clean solution was measured through the SECOMAN brand UV-vis spectroscopy. After each experiment, the biochar/Fe_3O_4 composite was washed several times using deionized water to be reuse. All experiments were triplicated to ensure the consistency and reproducibility of the results. The MB degradation percentage is calculated using Equation-4 below.

$$\% R = \frac{(Co-Ce).100}{Co} \quad (4)$$

Where: Co (mg/L) is the initial MB concentration, Ce (mg/L) is the MB concentration at equilibrium and % R is the MB degradation percentage.

Results and Discussion

Characterization: Fourier transformed infra-red analysis: The FTIR analysis was done to determine the structural characterization of PB_1P_1 and PB_1P_1M. The spectra are depicted in Figure-1 below.

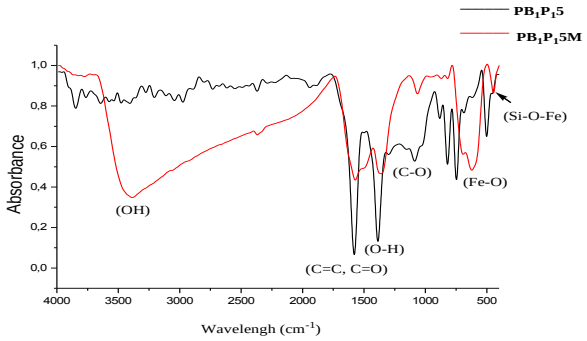

Figure-1: FTIR spectra of PB1P15 and PB1P15M.

The FTIR spectra of PB_1P_15 and PB_1P_15M showed several bands, some of which corresponding to the (-OH) elongation vibration of water molecules, acids or alcohols around 3500-3250cm^{-1}. Concerning the biochar composite (PB_1P_15), these bands are less intense, due to the fact that activation at 500^{0}C promotes the evaporation of certain compounds such as water. This band reappeared very intense on the magnetized biochar/magnetite composite (PB_1P_15M) may be due to the synthesis mode used which was by co-precipitation of $FeCl_3.6H_2O$ and $FeCl_2.4H_2O$ aqueous medium. The C=C and C=O groups elongation bands were found in the range 1630-1530cm^{-1}, that of PB_1P_15M being the less intense band. The band around 1400-1300cm^{-1} was attributable to the (-OH) deformation vibrations of water molecules. The presence of another less intense band around 1100-1039 cm^{-1} was due to the C-O vibration bonds of acids, alcohols and ethers. All the peaks in the interval 834-735cm^{-1} can be attributed to the Si-O bonds of elongation and valence vibrations. Aroke et al. in their study on the FTIR characterization of kaolin, granite, bentonite and barite have detected the same band[17] between 800-795cm^{-1}. Finally, the band corresponding to the C-H deformation bonds of aromatic group was located at 520-440cm^{-1} with, two additional bands observed on FTIR spectrum of PB_1P_15M as presented in Figure-1. A more intense band at 640-580cm^{-1} was detected and corresponding to Fe-O elongation vibration of iron oxides and the other less intense around 460-420cm^{-1}, attributed to Si-O-Fe vibration of the iron oxide and silica[18].

SEM-EDX Analysis: The SEM-EDX analysis of the PB_1P_15 and PB_1P_15M materials are presented in Figure-2. The micrographs analysis showed few visible and net channels on PB_1P_15 surface (a) and not on PB_1P_15M surface (c). This lack of visible and real channels on PB_1P_15M surface may be the consequence of obstruction of these channels by iron oxides detected (Figure-4d) and which were fixed on the surface of biochar composite during the synthesis process[19]. The information on the elemental composition of the two synthesized materials are compiled in Table-1. It can be noticed that several elements had low molecular weight, independently of the synthesis mode and materials synthesized. Also, it can be seen a slightly decrease in the carbon percentage and inversely it can be observed a slightly increase in the oxygen level from PB_1P_15 to PB_1P_15M that variation occurred during co precipitation step. The absence and presence of iron in PB_1P_15 and PB_1P_15M composition respectively and additionally as the third most abundant element confirmed that iron oxides have really been formed on PB_1P_15M. The presence of iron on PB_1P_15M surface was consisted to the assumption made of obstruction of channels by iron oxides.

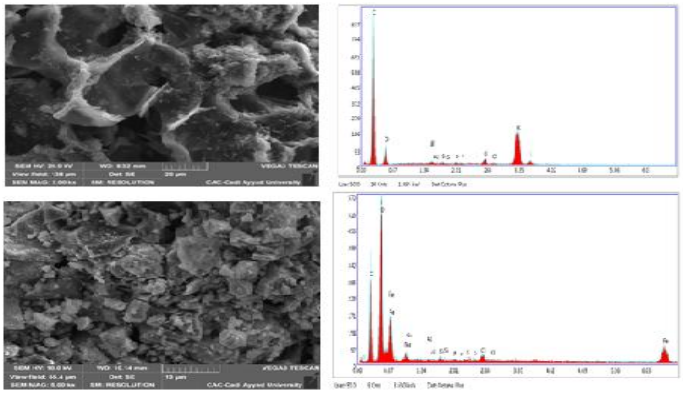

Figure-2: Micrographs and elemental composition EDX for PB1P15 (a and b) and PB1P15M (c and d).

Table-1: Elemental composition of PB_1P_15 and PB_1P_15M.

Material name	Elements	Weight (%)	Percentage of atoms (%)	Material name	Elements	Weight (%)	Percentage of atoms (%)
PB_1P_15	C	50.09	70.74	PB_1P_15M	C	30.28	44.65
	O	11.60	12.28		O	40.00	44.28
	Fe	0	0		Fe	23.66	7.51
	Al	0.67	0.42		Al	0.21	0.14
	Si	0.64	0.38		Si	0.63	0.40
	P	0.78	0.42		P	0.58	0.33
	Cl	3.46	1.65		Cl	2.63	1.31
	K	32.76	14.19		S	0.81	0.45
	Na	0	0		Na	1.21	0.93
	Total	100	100		Total	100	100

BET/BJH analysis: The N_2 adsorption / desorption analysis carried out on materials, indicates weak adsorption of N_2 at relative pressures P/P0< 0.01 indicating very few micropores on their surfaces. On the other hand, their curves are similar to the type IV isotherm characteristic of adsorbent shaving a very narrow distribution of mesopores according IUPAC (Figure-3). These are associated with hysteresis loops corresponding to tubular pores of almost constant section open at both ends. Nevertheless, these materials present some parallel portions to the ordinate axis at low pressure also reflecting the presence of micropores on their surfaces. However, despite the heterogeneous nature of the surface of ours samples, the average radius are 8.3738 and 4.3805nm for PB_1P_15 and PB_1P_15M respectively confirm their mesoporosity.

The two basic materials have specific surfaces areas of 83.03 m^2/g to 163.9m^2/g for biochar (PB_1P_15) and diochar/Fe_3O_4 (PB_1P_15M) respectively. These results indicate that, the ferromagnetic effects on biochars can considerably increase their specific surfaces from simple to double. These results are in line with other previous studies[20].

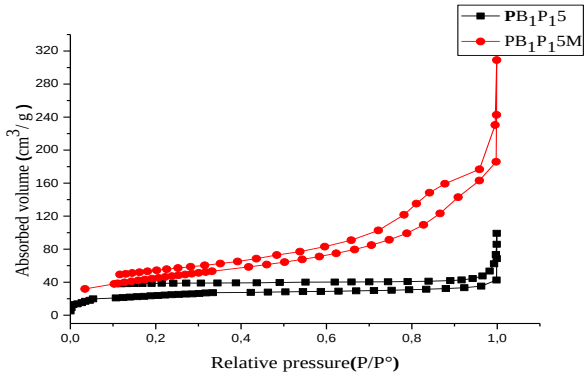

Figure-3: The N_2 adsorption/desorption isotherms.

Fenton and photo-Fenton degradation analysis: In order to evaluate the performance of the two composite materials prepared, simple adsorption, catalytic and photocatalytic degradation studies have been performed. The degradation percentage against the time has been sketched and given by the graph of in Figure-4. The adsorption of 80mg/L of MB aqueous solution onto PB_1P_15, PB_1P_15M and Fe_3O_4 using 15mg of each material was evaluated at pH value of 2, with 60 and 90 min of stirring times. The adsorption capacities obtained were 2.5 and 18% for Fe_3O_4, PB_1P_15 and PB_1P_15M materials respectively. These low adsorbed quantities may be to strong electrostatic repulsive that occurred between positively surface charged of materials and the cationic MB ions. Moreover, the Fenton process analysis using Fe_3O_4/H_2O_2 and PB_1P_15M/H_2O_2 by adding 0.2mg/L of H_2O_2 in a dark condition increased MB degradation percentage from 65.5 to 96.4% for Fe_3O_4/H_2O_2 and PB_1P_15M/H_2O_2 respectively. This important increase of degradation percentage of MB compared to that obtained previously with Fe_3O_4, PB_1P_15 and PB_1P_15 M may certainly be due to the addition of H_2O_2 solution, which of course was a source of very reactive $HO^{\bullet}$ radicals for Fenton reactions[11]. Crossing from the Fenton process (dark condition) to the photo-Fenton process (UV-light condition), it was noticed that the MB degradation percentage yielded up to 98.4 % for PB_1P_15M/H_2O_2 after 60 min of exposure to UV-light in the same adsorption condition of 0.2mL/L of H_2O_2, 15mg of catalyst at pH value of 2. This exponential increase of MB degradation percentage could be attributed to the biochar which according to Teguh et al. could reduce the energy gap of the iron thus facilitating the transfer of electrons from the valence band to the conductance band[10]. This process would likewise prevent the recombination of electron holes during the photocatalytic process. Finally, UV irradiation aimed at increasing the production of free radicals by stimulating the reduction of Fe^{3+} to Fe^{2+} (Equation-3), thus increasing the degradation rate of organic pollutants such as MB[7].

The pH value is recognized as an important parameter during photocatalysis process, because the percentage of degradation varies with the change in the pH value of solution. The effect of pH value was studied for pH 2 and pH 3 with the following adsorption conditions: 80mg/ L of MB solution, 0.2mL/L of H_2O_2, 60 min of contact time. The Figure-5 showed that the MB degradation percentage increased with time for both pH values studied. At pH = 2, MB degradation percentage was yielded to 98.4%, whereas it dropped to 88.5% at pH = 3. This could be explained by the fact that at the beginning of the process, maybe there was a completion between Fe^{2+} or Fe^{3+} complexes formation as well as iron oxyhydroxides sedimentation at pH = 3. These reasons could reduce the number of Fe^{2+} ions available and decreased oxidation potential of $HO^{\bullet}$ by inducing low photocatalytic activity of MB. While at pH = 2, the Fe^{3+} ions were mainly in the form of $Fe(OH)^{2+}$. These species absorbed UV- light in wavelength region of $250 < \lambda < 400$nm significantly better than the Fe^{3+} ions. The photochemical reduction of $Fe(OH)^{2+}$ in aqueous solution firstly allowed the production of additional $HO^{\bullet}$ radicals, and secondly catalyzed the Fenton reaction through the regeneration of Fe^{2+} ions according to Equations-8 to 10. The MB degradation is not obvious at high pH values due to the instability of hydrogen peroxide (H_2O_2) in alkaline solution and the production of $HO^{\bullet}$ radicals at the surface of the catalysts gradually decreased as the pH value increased.

$$H_2O_2 + Fe^{2+} + H^+ \longrightarrow Fe^{3+} + H_2O + {}^{\circ}HO \quad (8)$$
$$Fe^{3+} + H_2O \longrightarrow Fe(OH)^{2+} + H^+ \quad (9)$$
$$Fe(OH)^{2+} + h\upsilon \longrightarrow Fe^{2+} + {}^{\circ}HO \quad (10)$$

Effects of catalyst amount of and exposure time: To study the effects of catalyst mass and exposure to UV-light, experiments have been performed using the following condition: catalyst masses ranging from 6 to 15mg; pH = 2, 0.2mL/L H_2O_2, 50mL of MB 80mg/L and for 60 and 90 min of reaction time. Figure-8 illustrated the MB degradation versus catalyst masses. The analysis of obtained results showed that the catalytic and photocatalytic degradation gradually increased with catalyst mass until an establishment of plateau for 15mg of catalyst mass. This could be due to the increase in the number of active sites on catalyst as its mass rises. In dark condition, MB degradation reached 88.5% for a maximum catalyst mass of 15mg, after 60 min and 96.4% after 90 min. Moreover, when the mixture is exposed to UV-light MB degradation yielded 98.4% under the same conditions in 60 min of reaction time. The less decolorization capacity of Fe^{2+} observed at lower catalyst mass maybe attributed to the low hydroxyl radical's production. Therefore, increasing catalyst mass from 5 to 15mg resulted in an increase of decolonization of the MB solution. It is obvious that large quantities of radicals are produced by increasing Fe^{2+} ions concentration which is illustrated by Equation-17. The graphs of Figure-6 depicted the MB degradation under dark and UV-light conditions versus time for different masses. It can be noticed that, an increase of degradation rate when the contact time increased. For a reaction time of 60 min in dark condition, the degradation percentage of 88.5, 81.21 and 69.7% for 15, 10 and 5mg catalyst mass are obtained respectively. For the same contact time, but in UV-light condition, the degradation percentages obtained were 98.4, 95.5 and 87.27% for the same masses above. The degradation percentage for catalyst mass of 15 mg in UV-light condition were 45.5, 89.7, 95.7 and 98.4% and 4.9, 28, 49 and 88.5% in the dark condition for 15, 30, 45 and 60 min of contact time of respectively. This gradual increase observed in degradation percentage with increasing time maybe be due to continuous production of $HO^{\bullet}$ radicals on photocatalyst surface.

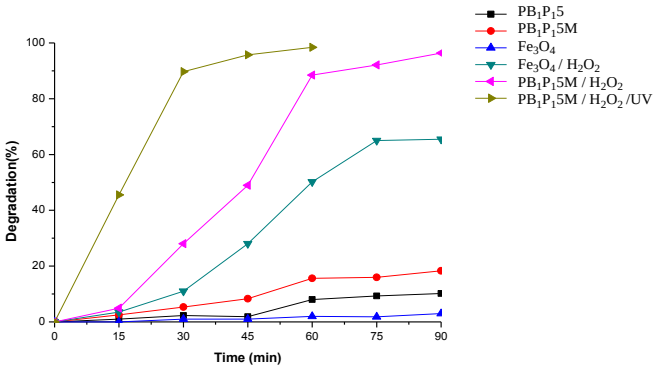

Figure- 4: Graph of MB degradation versus time on different materials (80 mg/L of MB solution, 0.2mL/L of H_2O_2, and pH = 2).

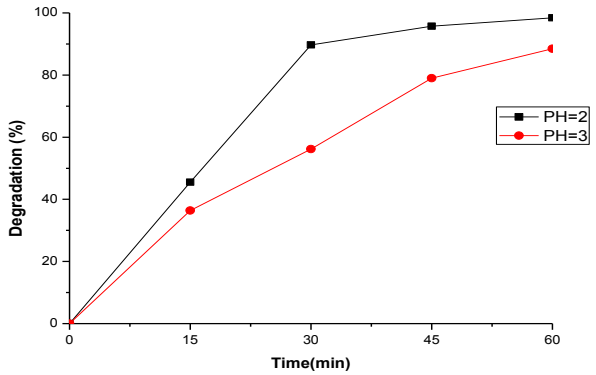

Figure-5: Graph of MB degradation versus time for the two pH values (80mg/L of MB, 15mg of PB_1P_15M, 0.2mL/L H_2O_2 in UV- light condition).

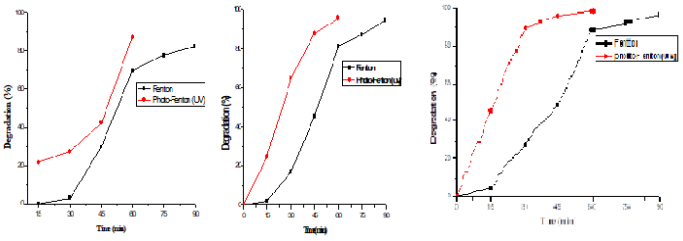

Figure-6: Effect of catalyst masses, 5mg (a); 10mg (b) and 15mg (c) (pH 2, 0.2mL/L of H_2O_2, 80mg/L of MB).

Absorption spectrum analysis: The adsorption spectra of the MB solution as a function of time depicted in Figure-7 were recorded in the range 200-800nm for 80mg/L of MB concentration, pH=2, 0.2mL/L of H_2O_2, and 15mg of PB_1P_15M/H_2O_2 catalyst mass. The MB degradation was observed after 60 min and 90min under UV- light and dark condition respectively. It observed was at the end a virtual disappearance of adsorption spectra in UV-visible domains. This disappearance was faster in UV-light accompanied with subsequent destruction of chromophore responsible of MB color. This observation reflected that MB benzene ring and heteropolyaromatic linkages were likely destroyed hence MB completely degraded[21].

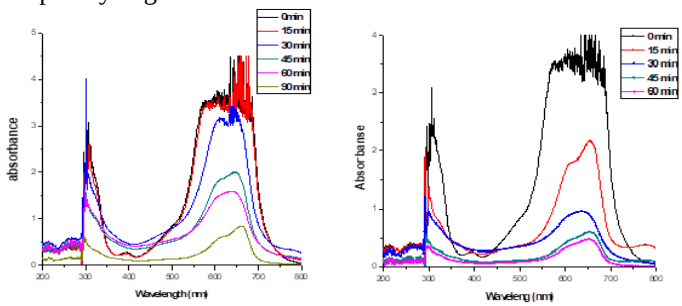

Figure-7: UV-visible spectral variation for different time of MB degradation: Fenton (a) and photo-Fenton (b) processes (15mg PB_1P_15M, 0.2mL/L of H_2O_2, pH = 2 and 25^0C).

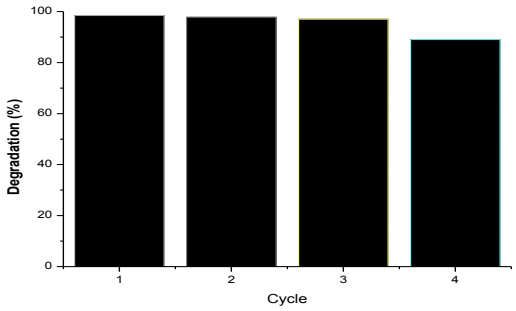

Figure-8: Cycles of catalyst material recycling (for 50mL solution of 80mg / L MB, 15mg PB_1P_15M, 0.2mL/L of H_2O_2 UV- light condition).

Stability and reusability of exhausted catalyst: The possibility of regeneration and reuse of the material have been studied and the MB degradation percentage values were regrouped in Figure-8. After recovering PB_1P_15M by magnetic filtration, it was suggested to washing several times with distilled water, dried and reused for four cycles. During the first three cycles, PB_1P_15M showed its effectiveness; by remaining stable. The decrease in activity was observed in the fourth cycle with a loss estimated at 9.4% degradation percentage compared to the first recycling. These results of regeneration tests confirmed that PB_1P_15M be used recovered and reused three times with a less loss of activity.

Conclusion

An efficient catalyst material, PB_1P_15M, have been synthesized by co-precipitation technique using biochar derived from banana peels and plastic bottles. The catalyst showed good physicochemical and electrochemical properties. These characteristics have used to MB degradation in dark and UV-light conditions. MB degradation percentages of 88.5% and 98.4% have been obtained for dark and UV-light conditions respectively. PB_1P_15M showed high photocatalytic efficiency and good reuse with a less loss of activity within three repetitive recycling. It had been demonstrated that MB degradation mechanism was initiated by H_2O_2/UV presence which produces $HO^{\bullet}$ radicals responsible of the attack MB benzene ring and heteropolyaromatic linkages. Finally, the catalyst so synthesized could play an important role in the complete degradation of recalcitrant dyes in wastewaters streams.

Acknowledgment: The authors are grateful to the Laboratory of Applied Organic Chemistry and the "Semlalia-Marrakech Analysis and Characterization Center", Faculty of Science Semlalia, Cadi Ayyad University (Morocco), where all the experiments and analyses have been carried out.

References

1. Mukhlish M.Z.B., Khan M.M.R., Islam A.R. and A.N.M.S (2016). Akanda1 Removal of reactive dye from aqueous solution using coagulation–flocculation coupled with adsorptionon papaya leaf. *Journal of Mechanical Engineering and Sciences*, 10, 1884, 1894.
2. Abid A.F., Zablouk M.A. and_ Abid-Alameer A.M. (2012). Experimental study of dye removal from industrial wastewater by membrane technologies of reverse osmosis and nanofiltration. *Iranian Journal of environmental Health Science* & *Engineering*, 9, 1-9.
3. Nasrollahpour A. and Moradi S.E. (2015). Photochemical degradation of methylene blue by metal oxide-supportedactivated carbon photocatalyst. *Desalination and Water Treatment*, 1-9.
4. Yu S., Liu M., Ma M., Qi M., Lü Z. and Gao, C. (2010). Impacts of membrane properties on reactive dye removal from dye/salt mixtures by asymmetric cellulose acetate and composite polyamide nanofiltration membranes. *Journal of Membrane Science*, 350, 83–91.
5. Chen B., Cao Y., Zhao H., Long F., Feng X., Li J. and Pan X. (2010). A novel Fe^{3+}-stabilized magnetic polydopamine composite for enhanced selective adsorption and separation of Methylene blue from complex wastewater. *Journal of Hazardous Materials*, 392, 1-15.
6. Kim, S. D.; Cho J.; Kim I. S.; Vanderford, B. J. and Snyder S. A. (2007). Occurrence and removal of pharmaceuticals and endocrine disruptors in South Korean surface, drinking, and waste waters. *Water Research*, 41, 1013−1021.

7. Zaviska F., Drogui P., Mercier G. and Blais J-F. (2009). Procédésd'oxydationavancée dans le traitement des eaux et des effluents industriels: Application à la dégradation des polluantsréfractaires. *Revue des Sciences de l'Eau*, 22, 535-564.

8. Aboel-Magd A-W., Al-Sayed A-S., Omima M. and Osama N. (2017). Photocatalytic degradation of paracetamol over magnetic flower-like TiO_2/Fe_2O_3 core-shell nanostructures. *Journal of Photochemistry and Photobiology A Chemistry*, 347, 186-198.

9. Khan M. R., Asw K. and Fahmida G. (2015). Photocatalytic Degradation of Methylene Blue by Magnetite+H_2O_2+UV Process. *International Journal of Environmental Science and Development*, 7, 325-329.

10. Kai Z., Jubo Z., Yan W., Longxue G., Mingyu D., Fang Y., Wenhui B., Tao Y. and Daxin L. (2018). Photo-Fenton Degradation of Organic Dyes Based on a Fe_3O_4 Nanospheres/Biomass Composite Loaded Column. *Journal of Nanoscience and Nanotechnology*, 18, 4288-4295

11. Teguh E.S., Oktaviana D.I.P., Abu M.N.H. and Miftahul A. (2016). The Modification of Carbon with Iron Oxide Synthesized in Electrolysis Using the Arc Discharge Method. *Materials Science and Engineering*, 176, 1-6.

12. Jong-Hwan P., Jim J. W., Ran X., Negar T., Ronald D. D. and Dong-Cheol S.(2017). Degradation of Orange G by Fenton-like reaction with Fe-impregnated biochar catalyst. *Bioresource Technology*. doi:10.1016/j.biortech.2017.10. 030.

13. Md Manik M. and Guijian L. (2018). Recent progress in biochar-supported photocatalysts: synthesis, role of biochar, and applications. *The Royal Society of Chemistry*, 8, 14237–14248.

14. Poedji L.H., Muhammad F., Ridwan, M. and DediS. (2013). Synthesis and Properties of Fe_3O_4 Nanoparticles by Co-precipitation Method to Removal Procion Dye. *International Journal of Environmental Science and Development*, 4, 336-340.

15. Shalini G. and Saima H. K. (2016). Removal of methylene blue from waste water using banana peel as adsorbent. *International Journal of Science, Environment*, 5, 3230-3236.

16. Monika J., Mithilesh Y., Tomas K., Manu L., Vinod K.G and Mika S. (2018). Development of iron oxide/activated carbon nanoparticle composite for the removal of Cr(VI), Cu(II) and Cd(II) ions from aqueous solution. *Water Resources and Industry*, 1-59. doi:10.1016/j.wri.2018.10. 001

17. Aroke U.O., Abdulkarim A. and Oaubunka R.O. (2013). Fourier-transform infrared characterization of kaolin, granite, bentonite and barite. *ATBU Journal of environnemental technology*, 6, 42-53.

18. Fatemeh A., Ali H. and Sirous N. (2013). Surface modification of $Fe_3O_4@SiO_2$ microsphere by silane coupling agent. *International nano letters*, 3, 1-5

19. Zhang, J., Fan S., Lu B., Cai Q., Zhao J. and Zang S. (2019). Photodegradation of naphthalene over Fe_3O_4 under visible light irradiation. *Royal Society Open Science*, 6, 181779, 1-14. doi:10.1098/rsos.181779.

20. Cristina T. F. Leonardus F.S., Vergütz L., Pacheco A.A., Melo L.F., Renato N.S. and Melo L.C.A. (2020). Characterization and application of magnetic biochar for the removal of phosphorus from water. *Annals of the Brazilian Academy of Sciences*, 3, 1-13.doi 10.1590/0001-3765202020190440.

21. Lincheng Z., Yanming S., Junrui L., Zhengfang Y., He Z., Junjun M., Yan J., Weijie G. and Yanfeng L. (2014). Preparation and Characterization of Magnetic Porous Carbon Microspheres for Removal of Methylene Blue by a Heterogeneous Fenton Reaction. *Applied Materials and Interfaces*, 6, 7275−7285.